

# Sum-Rate Analysis for 3D MIMO with ZF Receivers in Ricean/Lognormal Fading Channels

Fangqing Tan<sup>1</sup>, Hui Gao<sup>1</sup>, Xin Su<sup>2</sup> and Tiejun Lv<sup>1</sup>

<sup>1</sup>School of Information and Communication Engineering

<sup>1</sup>Beijing University of Posts and Telecommunications, Beijing, China 100876

<sup>2</sup>Tsinghua National Laboratory for Information Science and Technology

<sup>2</sup>Tsinghua University, Beijing, China 100084

[e-mail: {tfqing, huigao, lvtiejun}@bupt.edu.cn, suxin@tsinghua.edu.cn]

\*Corresponding author: Tiejun Lv

*Received January 30, 2015; revised May 19, 2015; accepted June 13, 2015;  
published July 31, 2015*

---

## Abstract

In this paper, we investigate the performance evaluation of three dimensional (3D) multiple-input multiple-output (MIMO) systems with an adjustable base station (BS) antenna tilt angle and zero-forcing (ZF) receivers in Ricean/Lognormal fading channels. In particular, we take the lognormal shadow fading, 3D antenna gain with antenna tilt angle and path-loss into account. First, we derive a closed-form lower bound on the sum rate, then we obtain the optimal BS antenna tilt angle based on the derived lower bound, and finally we present linear approximations for the sum rate in high and low-SNR regimes, respectively. Based on our analytical results, we gain valuable insights into the impact of key system parameters, such as the BS antenna tilt angle, the Ricean  $K$ -factor and the radius of cell, on the sum rate performance of 3D MIMO with ZF receivers.

---

**Keywords:** 3D MIMO, Ricean fading, Lognormal shadow fading, ZF receivers, Lower bound, Low/High-SNR approximation.

---

This work is supported by the National Natural Science Foundation of China (NSFC) (Grant No. 61271188, 61401041), the Fundamental Research Funds for the Central Universities (Grant No. 2014RC0106), Beijing Municipal Science and Technology Commission Research Fund Project (Grant No. D151100000115002), National S&T Major Project (Grant No. 2014ZX03004003), and China 863 Project (Grant No.2014AA01A707).

## 1. Introduction

Multiple-input multiple-output (MIMO) technology can significantly improve the transmission data rate and reliability of wireless communication systems without requiring extra bandwidth or transmit power [1]. In particular, multi-user MIMO (MU-MIMO) systems, where a multi-antenna base station (BS) serves a number of users in the same time-frequency resource, have gained substantial interest for the spatial multiplexing gains [2]. Currently, most existing studies on MU-MIMO techniques mainly focus on two-dimensional (2D) channel model only consider the horizontal dimension of the BS antenna pattern. They ignore the effect of elevation in the vertical dimension. To make the channel model more practical, three-dimensional (3D) channel is introduced. In the existing 3D-MIMO models, an approximated 3D radiation pattern is used to address the antenna tilt angle in vertical planes [3-5].

An important topic in MU-MIMO communication theory is to obtain theoretical results of the system sum rate. Unfortunately, many of the existing works focus only on the simple Rayleigh fading channels [6-8]. However, many realistic channels are characterized by a deterministic or line-of-sight (LoS) component. In such scenarios, Ricean fading channel model is more useful and practical [9]. The sum rate of MIMO system with Ricean fading has been discussed in [10-13]. An analytical framework of the capacity was provided for uncorrelated Ricean fading MIMO channels in [10]. In [11, 12], several upper and lower bounds were provided for uncorrelated Ricean fading MIMO system, where the transmitter has knowledge of statistical properties of the fading channel but not the instantaneous channel state information (CSI). In [13], the sum rate analysis of MIMO systems with minimum mean-squared error (MMSE) was performed, some simplified closed-form expressions for the achievable sum rate were derived in the asymptotic regimes of high and low signal-to-noise ratios (SNR). Unfortunately, in above mentioned studies, only small-scale fading was considered; little attention was paid to the realistic effect of large-scale fading, mainly due to the difficulty in analyzing the statistical distribution of large-scale fading. Furthermore, in practical scenarios, the distribution of the large-scale fading might largely vary in different scenarios, such as urban and open areas. The study on the effect of the large-scale fading in MIMO system is still open. Motivated by this fact, in this paper we focus on investigating the performance analysis of the 3D-MIMO system over composite fading channels including the path-loss, the lognormal (LN) shadow fading and 3D antenna gain.

In this paper, we introduce a general analytical framework for investigating the sum rate of Ricean/lognormal (RC-LN) 3D-MIMO systems with ZF receivers by exploiting BS antenna tilt angle. We derive a lower bound sum rate expression for the whole SNR regime, and further study the asymptotic approximation of the sum rate to gain more insights. Moreover, the optimal BS antenna tilt angle is investigated for maximizing the system sum rate. Simulation results show that the derived lower bound and high/low-SNR approximations are applicable to arbitrary Ricean  $K$ -factor and remain relatively tight across the entire BS antenna tilt angle range and SNR regimes. Our analytical results are quite informative and insightful to characterize the impact of the shadow fading, the Ricean  $K$ -factor, the BS antenna tilt angle and the path-loss on the system sum rate.

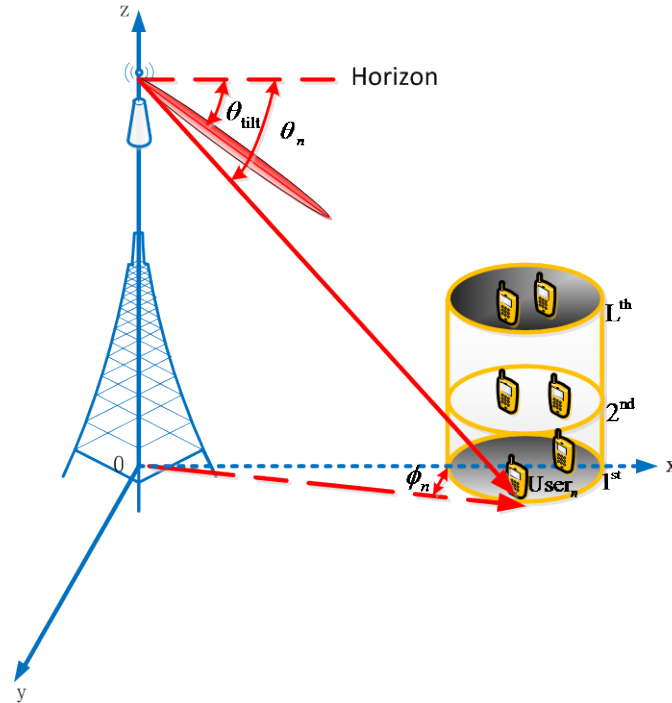


**Fig. 1.** A 3D-MIMO system with  $N$  users located in an  $L$ -floor building.

The rest of the paper is organized as follows. In Section 2, we specify the 3D-MIMO system model. In Section 3, we derive the lower bounds, low/high-SNR approximations of the system sum rate and the optimal BS antenna tilt angle. In Section 4, the numerical results are shown with discussion. Finally, we conclude in Section 5.

*Notations:* For a matrix  $\mathbf{A}$ ,  $\text{tr}(\mathbf{A})$ ,  $\mathbf{A}^H$ ,  $\mathbf{A}^T$ , and  $\mathbf{A}^\dagger$  denote the trace, conjugate transpose, transpose, and pseudo inverse of  $\mathbf{A}$ , respectively. The symbol  $CN(\mathbf{M}, \mathbf{\Sigma})$  denotes a complex Gaussian matrix with mean  $\mathbf{M}$  and covariance  $\mathbf{\Sigma}$ . The  $(i, j)^{\text{th}}$  entry of matrix  $\mathbf{A}$  is denoted by  $[\mathbf{A}]_{i,j}$ , while  $\mathbf{A}_i$  is  $\mathbf{A}$  with  $i^{\text{th}}$  column removed. The symbol  $E[\ ]$  stands for the expectation operation. The symbol  $\Gamma(\ )$  stands for the Gamma function,  $\psi(\ )$  is Euler's digamma function, and  $E_i(\mathbf{x}) = \int_{-\infty}^{\mathbf{x}} \frac{e^t}{t} dt$  is the exponential integral function. Finally,  ${}_pF_q(\ )$  is the generalized hyper-geometric function with  $p, q$  non-negative integers [14].

## 2. 3D-MIMO System Model

### 2.1 Channel Model

Considering an uplink single-cell MU-MIMO system depicted in Fig. 1, the system consists of a BS equipped with  $M$  antennas that receive data from  $N$  single-antenna users. It is assumed that  $M \geq N$ . The users transmit their data in the same time-frequency resource. All users are distributed in an  $L$ -floor building. For the sake of effective analysis, the floor penetration loss and the surface reflection loss are not taken into account. Assuming no CSI at the transmitters,

the available average transmit power  $P$  is distributed uniformly amongst all data streams. Then, the  $M \times 1$  received signal vector at the BS is

$$\mathbf{y} = \sqrt{\frac{P}{N}} \mathbf{G} \mathbf{s} + \mathbf{n}, \quad (1)$$

where  $\mathbf{G} \in \mathbb{C}^{M \times N}$  is the MIMO channel matrix between the BS and the  $N$  users,  $\mathbf{s} \in \mathbb{C}^{N \times 1}$  is the vector containing the transmitted symbols of the  $N$  users which are drawn from a zero-mean Gaussian codebook with unit average power. And  $\mathbf{n} \in \mathbb{C}^{N \times 1}$  is the complex additional white Gaussian noise (AWGN) vector, such that  $CN(0, N_0 \mathbf{I}_N)$ .

The channel matrix  $\mathbf{G}$  includes independent small- and large-scale fading, it can be expressed by

$$\mathbf{G} = \mathbf{H} \mathbf{\Xi}^{1/2}, \quad (2)$$

where  $\mathbf{H} \in \mathbb{C}^{M \times N}$  is the small-scale fading between the  $N$  users and the BS. In Ricean fading channel, the entries of  $\mathbf{H}$  are nonzero mean complex Gaussian random variables (RVs), it consists of two parts, namely, a deterministic component  $\mathbf{H}_L$  corresponding to the LoS signal and a Rayleigh distributed random component  $\mathbf{H}_\omega$  accounting for the scattered signals.  $\mathbf{H}$  can be written as

$$\mathbf{H} = \sqrt{\frac{K}{K+1}} \mathbf{H}_L + \sqrt{\frac{1}{K+1}} \mathbf{H}_\omega, \quad (3)$$

where  $K$  stands for the Ricean  $K$ -factor, it denotes the ratio between the deterministic (specular) and the random (scattered) energies. The term  $\mathbf{H}_L$  is typically associated with a LoS or a diffracted component and thus, assuming far field transmission, it can be expressed as

$$\mathbf{H}_L = \mathbf{a}_r(\theta_r) \mathbf{a}_t(\theta_t)^T, \quad (4)$$

where  $\mathbf{a}_r(\theta_r) = [1, e^{j2\pi d \cos(\theta_r)}, \dots, e^{j2\pi d(M-1)\cos(\theta_r)}]^T$  and  $\mathbf{a}_t(\theta_t) = [1, e^{j2\pi d \cos(\theta_t)}, \dots, e^{j2\pi d(N-1)\cos(\theta_t)}]^T$  are the specular array response at the receiver and transmitter, respectively, and  $d$  is the antenna spacing in wavelengths,  $\theta_r, \theta_t$  are the angles of arrival and departure of the specular component, respectively. The scattered component of  $\mathbf{H}$  is denoted by  $\mathbf{H}_\omega$ , where the entries of  $\mathbf{H}_\omega$  are independent and identically distributed (i.i.d)  $CN(0,1)$  RVs.

The diagonal matrix  $\mathbf{\Xi} \in \mathbb{R}^{N \times N}$  represents the large-scale fading and can be written as  $\mathbf{\Xi} = \text{diag}\{\beta_n(\theta_{\text{ilt}})\}_{n=1}^N = \text{diag}\{d_n^{-\nu} g_n(\theta_{\text{ilt}}) \xi_n\}_{n=1}^N$ , where  $d_n^{-\nu}$ ,  $g_n(\theta_{\text{ilt}})$  and  $\xi_n$  are the path-loss, the 3D antenna gain and the shadow fading coefficient corresponding to the  $n^{\text{th}}$  entry, respectively. The shadow fading coefficient  $\xi_n$  is modeled as an independent LN

random variable (RV), namely,  $\xi_n \sim \text{LN}\left(\frac{\mu_n}{\eta}, \frac{\sigma_n^2}{\eta}\right)$ , or

$$f_{\xi_n}(x) = \frac{\eta}{x \sqrt{2\pi\sigma_n^2}} e^{-\frac{(\eta \ln x - \mu_n)^2}{2\sigma_n^2}}, \quad (5)$$

where  $\eta = 10/\ln 10$ , while  $\mu_n$  and  $\sigma_n$  are the mean and standard deviation (both in dB) of the RV  $10 \lg \xi_n$ , respectively.

The considered channel model in (2) is a simplified 3D-MIMO model of the commonly used kathrein antenna 742215 [3]. To model the channel between the users and the BS, we assume that the height of the BS is much larger than that of the user. The antenna gain of the  $n^{\text{th}}$  user,  $g_n(\theta_{\text{tilt}})$  depends on the relative angles between the direct line from the user to the BS and the main lobe of the antenna pattern, both in horizontal (azimuth,  $\phi_n$ ) and vertical (elevation,  $\theta_n$ ) directions.  $(x_B, y_B, z_B)$  and  $(x_n, y_n, z_n)$  denote the coordinates of the BS and the  $n^{\text{th}}$  user, respectively. We denote  $\Delta x_n = x_n - x_B$  and  $\Delta y_n = y_n - y_B$  as relative distances between the  $n^{\text{th}}$  user and the BS in the x and y coordinate, respectively. Similarly,  $\Delta z_n = z_n - z_B$  is the height difference between the  $n^{\text{th}}$  user and the BS.

The distance between the  $n^{\text{th}}$  user and the BS is denoted as  $d_n$ , it can be calculated as

$$d_n = \sqrt{(\Delta x_n)^2 + (\Delta y_n)^2 + (\Delta z_n)^2}. \quad (6)$$

According to this model, the horizontal antenna radiation attenuation adopted by the 3GPP [3] is expressed in dB scale as

$$G_H(\phi_n) = \min \left\{ 12 \left( \frac{\phi_n}{\phi_{3\text{dB}}} \right)^2, A_m \right\}. \quad (7)$$

Similarly, the vertical antenna attenuation can be expressed in dB scale as

$$G_V(\theta_n, \theta_{\text{tilt}}) = \min \left\{ 12 \left( \frac{\theta_n - \theta_{\text{tilt}}}{\theta_{3\text{dB}}} \right)^2, A_m \right\}, \quad (8)$$

where  $\phi_n = \arctan(\Delta y_n / \Delta x_n)$  denotes the horizontal angle between the BS antennas boresight and the  $n^{\text{th}}$  user in the horizontal plane, and  $\theta_n = \arctan\left(\Delta z_n / \sqrt{(\Delta x_n)^2 + (\Delta y_n)^2}\right)$  indicates the vertical angle between the horizon and the line connecting the BS to the  $n^{\text{th}}$  user. In addition,  $\theta_{\text{tilt}}$  denotes the BS antenna tilt angle which is adjustable. Moreover,  $A_m$  represents the maximum attenuation of the BS antennas. The half-power beamwidth (HPBW) in the horizontal and vertical planes are denoted as  $\phi_{3\text{dB}}$  and  $\theta_{3\text{dB}}$ , respectively.

Let us denote  $G_m$  (in dB) as the maximum antenna gain at the antenna boresight. Then, after combining the antenna attenuation and the maximum antenna gain, the resultant antenna gain in dB scale for the  $n^{\text{th}}$  user with horizontal angle  $\phi_n$  and the vertical angle  $\theta_n$  can be formulated as

$$G_n(\theta_{\text{tilt}}) = G_m - \min \left\{ [G_H(\phi_n) + G_V(\theta_n, \theta_{\text{tilt}})], A_m \right\}. \quad (9)$$

The resultant antenna gain in the linear scale can be approximated as

$$10^{0.1G_n(\theta_{\text{tilt}})} \approx g_n(\theta_{\text{tilt}}) = 10^{0.1G_m - 1.2 \left( \frac{\phi_n}{\phi_{3\text{dB}}} \right)^2 - 1.2 \left( \frac{\theta_n - \theta_{\text{tilt}}}{\theta_{3\text{dB}}} \right)^2}. \quad (10)$$

The approximation is valid when  $G_H(\phi_n) + G_V(\theta_n, \theta_{\text{tilt}}) \leq A_m$  or  $A_m$  is large enough. For example, for the antenna model in [15],  $A_m$  is given as  $A_m = 20\text{dB}$ . In this case, the difference between  $10^{0.1G_n(\theta_{\text{tilt}})}$  and the approximated value  $g_n(\theta_{\text{tilt}})$  is less than 1%. The condition corresponds to the typical cell deployments.

With the LN shadow fading coefficient  $\xi_n$ , 3D antenna gain  $g_n(\theta_{\text{tilt}})$ , and distance dependent path-loss  $d_n^{-\nu}$ , the large-scale fading coefficient is finally expressed as

$$\beta_n(\theta_{\text{tilt}}) = \xi_n g_n(\theta_{\text{tilt}}) d_n^{-\nu}. \quad (11)$$

It is noteworthy that the large-scale fading  $\beta_n(\theta_{\text{tilt}})$  is treated as a random variable instead of a given value and in the following we will analyze the ergodic sum rate over  $\beta_n(\theta_{\text{tilt}})$ .

## 2.2 User Distribution Model

In the considered 3D-MIMO system, to analyze the collective behavior of users in the  $L$ -floor building, the building is approximated as a cylinder with a radius  $R$ , the height of floor-to-floor is set to be  $h_f$ . The radius of cell (i.e. the distance between BS and the center of the  $L$ -floor building) is  $D$ . We consider the horizontal distribution in each floor and vertical distribution in different floors.

For vertical distribution, it is modeled that users on different floors follow some rules. The user distribution is discrete. We assume the user number in the  $l^{\text{th}}$  floor is  $N_l$ , for  $l=1, \dots, L$ , and  $N = \sum_{l=1}^L N_l$ .

For horizontal distribution, we consider uniform distribution, i.e., the  $N_l$  users in the  $l^{\text{th}}$  floor are assumed to be i.i.d on the circular floor. The distribution of the users along the radius of the floor can be modeled as [16]

$$f_r(x) = \frac{2x}{R^2}, 0 \leq x \leq R. \quad (12)$$

## 3. Achievable Sum Rate of 3D-MIMO System with ZF Receivers

In this section, we firstly derive a closed-form lower bound on the sum rate of 3D-MIMO with ZF receivers. Furthermore, the optimal BS antenna tilt angle  $\theta_{\text{tilt}}^*$  is obtained to achieve maximum sum rate. Finally, the linear approximations are presented in high and low-SNR regimes, respectively.

We assume that BS has perfect CSI, i.e., it knows  $\mathbf{G}$ , then the ZF filter is expressed as

$\mathbf{A} = \left(\frac{P}{N}\right)^{\frac{1}{2}} \mathbf{G}^\dagger$  [17]. The instantaneous received SNR at the  $n^{\text{th}}$  ZF output ( $1 \leq n \leq N$ ) is [18]

$$\gamma_n(\theta_{\text{tilt}}) = \frac{\gamma}{N \left[ (\mathbf{G}^H \mathbf{G})^{-1} \right]_{n,n}} = \frac{\gamma [\mathbf{\Xi}]_{n,n}}{N \left[ (\mathbf{H}^H \mathbf{H})^{-1} \right]_{n,n}}, \quad (13)$$

where  $\gamma = \frac{P}{N_0}$  is the average transmit SNR. Note that the second equation follows from the fact that  $\mathbf{G} = \mathbf{H} \mathbf{\Xi}^{1/2}$ , and  $\mathbf{\Xi}$  is a diagonal matrix. The achievable sum rate is then determined as

$$\mathbf{R}(\theta_{\text{tilt}}, \gamma) = \sum_{n=1}^N \mathbf{E} \left[ \log_2 (1 + \gamma_n(\theta_{\text{tilt}})) \right]. \quad (14)$$

where the expectation  $\mathbb{E}[\ ]$  is taken over all channel realizations of  $\mathbf{H}$ ,  $\Xi$ . Due to randomness of small-scale fading  $\mathbf{H}$  and large-scale fading  $\Xi$ , it is difficult to obtain the exact expression of  $R(\theta_{\text{tilt}}, \gamma)$ . We circumvent this problem in the following by deriving some tractable bounds and approximations on the sum rate of 3D-MIMO system with ZF receivers.

### 3.1 Closed-form Bounds on the Achievable Sum Rate

In this subsection, we turn to derive a novel closed-form lower bound of the achievable sum rate of 3D-MIMO with ZF receivers. The key result is summarized in the following proposition.

**Proposition 1.** The achievable sum rate of 3D-MIMO ZF receivers in RC-LN fading channels is lower bounded by  $R_L(\theta_{\text{tilt}}, \gamma)$

$$R_L(\theta_{\text{tilt}}, \gamma) = \frac{1}{\ln 2} \sum_{n=1}^N \ln \left( 1 + \exp \left( \frac{\mu_n}{\eta} + \psi(M - N + 1) - \ln(K + 1) \right) \right) \times \frac{\gamma}{N} \exp(F(M, \Delta) - F(M, \Delta_1)) g_n(\theta_{\text{tilt}}) d_n^{-\nu}, \tag{15}$$

where  $\Delta = KMN$ ,  $\Delta_1 = KM(N - 1)$ , and

$$F(n, x) = \ln(x) - E_1(-x) + \sum_{k=1}^{n-1} \left( -\frac{1}{x} \right)^k \left( e^{-x} (k-1)! - \frac{(n-1)!}{k(n-k-1)!} \right). \tag{16}$$

**Proof:** Please see Appendix A.

**Remark 1:** It is easy to see that the lower bound of the sum rate monotonically grows with the mean of the LN shadow fading, and 3D antenna gain. We can get the maximum 3D antenna gain by optimizing the BS antenna tilt angle, and then obtain the maximum sum rate of 3D-MIMO system.

### 3.2 Optimization for the BS Antenna Tilt Angle

In this subsection, we aim to derive the optimal BS antenna tilt angle to maximize the sum rate in (14). Note that there are multiple random variables in (14), it is difficult to obtain a closed-form expression for (14) with clear physical insights. For tractability, we turn to optimize the BS antenna tilt angle regarding the lower bound of the sum rate in (15). The optimal BS antenna tilt angle is given by the following theorem.

**Theorem 1.** For 3D-MIMO systems with ZF receivers in RC-LN fading channel, the optimal BS antenna tilt angle  $\theta_{\text{tilt}}^*$  (regarding the lower bound) is the mean value of vertical

angles of the  $N$  users, i.e.,  $\theta_{\text{tilt}}^* \approx \sum_{n=1}^N \theta_n / N$ .

**Proof:** Please see Appendix B.

**Remark 2:** The optimal antenna tilt angle  $\theta_{\text{tilt}}^*$  can be easily obtained by averaging the vertical angles of the all users. No complicated calculation is required.

### 3.3 High SNR Analysis

In order to derive the diversity order of the system, we now analyze the sum rate performance in the high-SNR regime. We can invoke the affine sum rate expansion in the analysis of MIMO

systems [19] as follow:

$$R = S_\infty (\log_2(\gamma) - L_\infty) + o(1), \quad (17)$$

where  $S_\infty$  is the high-SNR slope in bits/s/Hz per 3-dB units, and  $L_\infty$  is the high-SNR power offset, in 3-dB units, given by

$$S_\infty = \lim_{\gamma \rightarrow \infty} \frac{R}{\log_2(\gamma)}, \quad L_\infty = \lim_{\gamma \rightarrow \infty} \left( \log_2(\gamma) - \frac{R}{S_\infty} \right). \quad (18)$$

**Proposition 2.** At the high SNR regime, the sum rate of 3D-MIMO with ZF receivers in RC-LN fading channel can be expressed with parameters in the general form (18) as follows

$$\begin{aligned} S_\infty &= N, \quad (19) \\ L_\infty &= \frac{1}{\ln 2} \ln(N) - \frac{1}{N \ln 2} \sum_{n=1}^N \ln(g_n(\theta_{\text{ult}}) d_n^{-\nu}) + \frac{\mu_n}{\eta} \\ &\quad - \frac{1}{\ln 2} (F(M, \Delta) - F(M, \Delta_1) - \ln(K+1) + \psi(M-N+1)). \end{aligned} \quad (20)$$

**Proof:** Please see Appendix C.

**Remark 3:** It can be observed that the  $S_\infty$  in (19) verifies that the high-SNR sum rate increases linearly with the minimum number of antennas, which agrees with [18]. From the  $L_\infty$  in (20), we can infer that the small and large-scale fading terms are decoupled in the high SNR regime. Furthermore, the greater the distances between the BS and users  $d_i$ , the much more effectively reduce the system sum rates due to the increased path-loss.

### 3.4 Low SNR Analysis

A wide variety of digital communication systems operate at low power where both spectral efficiency and the energy-per-bit can be very low. The low SNR analysis can provide a useful reference in understanding the system performance at low SNR regime. In this subsection, we examine the achievable sum rate at the low SNR regime. At low SNR, it has proved useful to investigate the sum rate of MIMO systems in terms of the normalized transmit energy per

information bit  $\frac{E_b}{N_0}$ , rather than the per-symbol SNR  $\gamma$  ( $\gamma = \frac{E_b}{N_0} R \left( \frac{E_b}{N_0} \right)$ ). At low-SNR, the

sum rate of MIMO systems can be well approximated for low  $\frac{E_b}{N_0}$  by the following expression

[19]

$$R \left( \frac{E_b}{N_0} \right) \approx \frac{S_0}{\ln 2} \ln \left( \frac{E_b}{N_0} / \frac{E_b}{N_{0 \min}} \right), \quad (21)$$

where  $\frac{E_b}{N_{0 \min}}$  and  $S_0$  are the minimum normalized energy per information bit required to convey any positive rate reliably and wideband slope, respectively. According to [20], these two key parameters can be obtained from  $R(\gamma)$  via



$$\frac{E_b}{N_{0 \min}} = \frac{1}{\dot{\mathbf{R}}(0)}, \quad \mathbf{S}_0 = -\frac{2 \ln 2 \left( \dot{\mathbf{R}}(0) \right)^2}{\ddot{\mathbf{R}}(0)}, \quad (22)$$

where  $\dot{\mathbf{R}}(0)$  and  $\ddot{\mathbf{R}}(0)$  denote the first- and second-order derivatives of the sum rate in (14) with respect to SNR (i.e.,  $\gamma$ ), respectively.

**Proposition 3.** For 3D-MIMO systems with ZF receivers in RC-LN fading channels, the minimum energy per information bit and the wideband slope are respectively given by

$$\frac{E_b}{N_{0 \min}} = \frac{\alpha N \ln 2}{M - N + 1} \left( \sum_{n=1}^N c_n \right)^{-1}, \quad (23)$$

$$\mathbf{S}_0 = \frac{2(M - N + 1) \left( \sum_{n=1}^N c_n \right)^2}{(M - N + 2) \left( \sum_{n=1}^N f_n \right)}, \quad (24)$$

where  $c_n = \exp\left(\frac{\mu_n}{\eta} + \frac{\sigma_n^2}{2\eta^2}\right) d_n^{-\nu} g_n(\theta_{\text{ult}})$ ,  $f_n = \exp\left(\frac{2\mu_n}{\eta} + \frac{2\sigma_n^2}{\eta^2}\right) d_n^{-2\nu} g_n^2(\theta_{\text{ult}})$ ,  $\alpha = \left[\hat{\Sigma}^{-1}\right]_{mm}$ .

**Proof:** Please see Appendix D.

**Remark 4:** It is clear to see that  $\frac{E_b}{N_{0 \min}}$  in (23) depends on the number of BS antennas  $M$ , the number of users  $N$ , the large-scale fading mean parameter  $c_n$  and the covariance matrix of  $\mathbf{H}$ ,  $\hat{\Sigma}$ . For fixed  $M$ , having more users is not beneficial for ZF receivers since the  $\frac{E_b}{N_{0 \min}}$  increases due to the additional power that is required to cancel out the exact interference. Note that the  $\mathbf{S}_0$  is by definition greater than one.

## 4. Numerical Results

In this section, we present various simulations to furtherly verify the derived analytical results. The BS is located at the origin of spatial coordinates. We assume that the users are located in the 3-floor building, the horizontal distribution is modeled as (12) and the vertical distribution is uniform, namely, the user number in each floor is equal,  $N_l = N/L$  for  $l = 1, \dots, L$ . We set the height of floor-to-floor  $h_f = 5\text{m}$ , the height of BS  $h_B = 30\text{m}$ , the radius of the floor  $R = 50\text{m}$ , the distance between the BS and the L-floor building  $D$  is variable. All the Monte-Carlo simulation results were obtained by averaging over  $1 \times 10^4$  independent channel realizations. For rank-1 Ricean fading MIMO channels, we assume  $\theta_r = \theta_t = \frac{\pi}{4}$ ,  $d = 0.5$ . The antenna parameters are set to be  $\theta_{3\text{dB}} = 6.2^\circ$ ,  $\phi_{3\text{dB}} = 65^\circ$ ,  $G_m = 20\text{dB}$ . Other channel parameters used in the simulations are set to be as follows: the path-loss exponent  $\nu = 4$ , the standard deviation of  $\xi_n$ ,  $\sigma_n = 2\text{dB}$ , the mean of  $\xi_n$ ,  $\mu_n = 4\text{dB}$ .

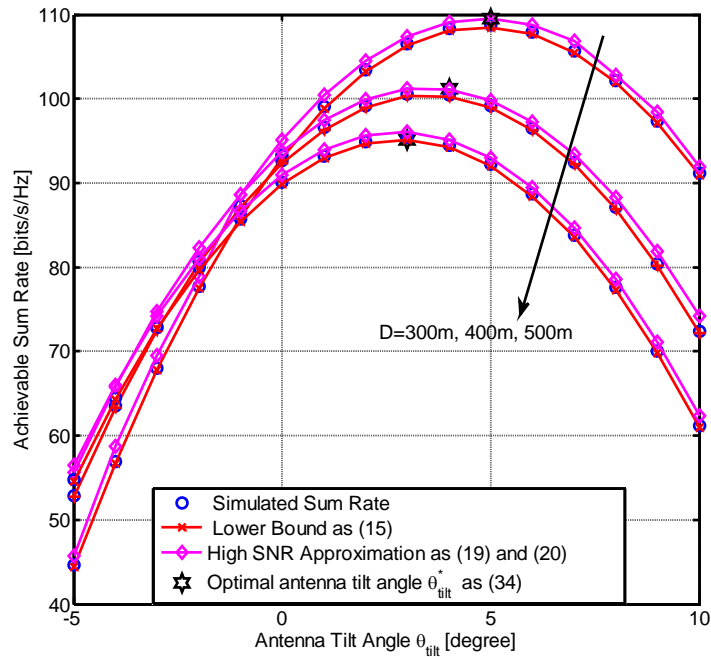


**Fig. 2.** Simulated sum rate, lower bound and high-SNR approximation versus the BS antenna tilt angle  $\theta_{\text{tilt}}$  in the high SNR regime ( $M = 10, N = 6, K = 1, \gamma = 20\text{dB}$ ).

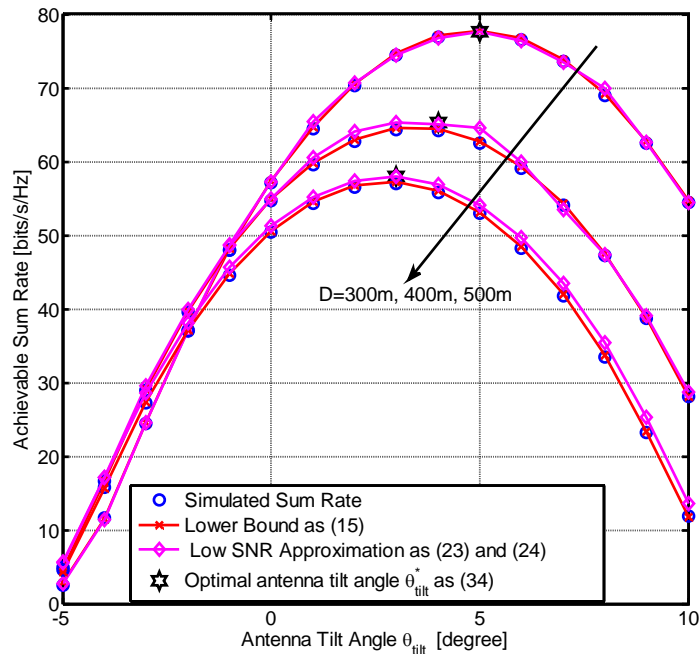


**Fig. 3.** Simulated sum rate, lower bound and low-SNR approximation versus the BS antenna tilt angle  $\theta_{\text{tilt}}$  in the low SNR regime ( $M = 10, N = 6, K = 1, \frac{E_b}{N_0} = -20\text{dB}$ ).

We firstly assess the sum rate performance of 3D-MIMO system against different parameters (the radius of cell  $D$ , the BS antenna tilt angle  $\theta_{\text{tilt}}$ ).

In **Fig. 2** and **Fig. 3**, the simulated sum rates of 3D-MIMO systems with ZF receivers are compared with their lower bounds, high-SNR approximations and low-SNR approximations, respectively. Results are presented for three different the radius of cell. In all cases, we can clearly see a precise match between the simulated results and the analytical results. At the same time, the radius of cell  $D$  also shows impact on the optimal BS antenna tilt angle  $\theta_{\text{tilt}}^*$ , which achieves the maximum sum rate of the system. More specifically, the sum rate increases with  $\theta_{\text{tilt}}$  before the optimal BS antenna tilt angle  $\theta_{\text{tilt}}^*$ , and then decreases with the  $\theta_{\text{tilt}}$  further increases since the radiation angle of the BS deviates from users.

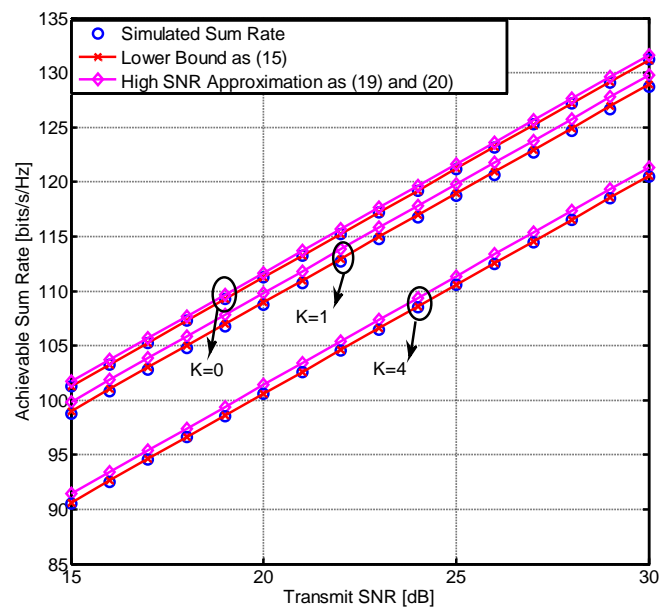


**Fig. 4.** Simulated sum rate, lower bound and high-SNR approximation versus the transmit SNR  $\gamma$  in the high SNR regime ( $M = 10, N = 6, D = 400, \theta_{\text{tilt}} = 4^\circ$ ).

To capture the effect of Ricean  $K$ -factor on the system sum rate, we further compared the simulated sum rate with their lower bounds, high and low-SNR approximations over different Ricean  $K$ -factor in the high and low-SNR regime in **Fig. 4** and **Fig. 5**, respectively. A quite good match between the simulated results and analytical results can be observed with various Ricean  $K$ -factors. The main observation is that a higher Ricean  $K$ -factor will decrease the system sum rate, since the specular components of channel increase, especially  $K = 0$  corresponds to the Rayleigh-fading. From the results of **Fig. 4**, we can observe that the simulated results are extremely accurate in comparison with the lower bounds and high-SNR approximations in the entire high SNR regime. In **Fig. 5**, it can be seen that the match of simulated results, lower bounds and low-SNR approximation is very good if the SNR of interest is sufficiently low (i.e., below 60 bits/s/Hz of sum rate).

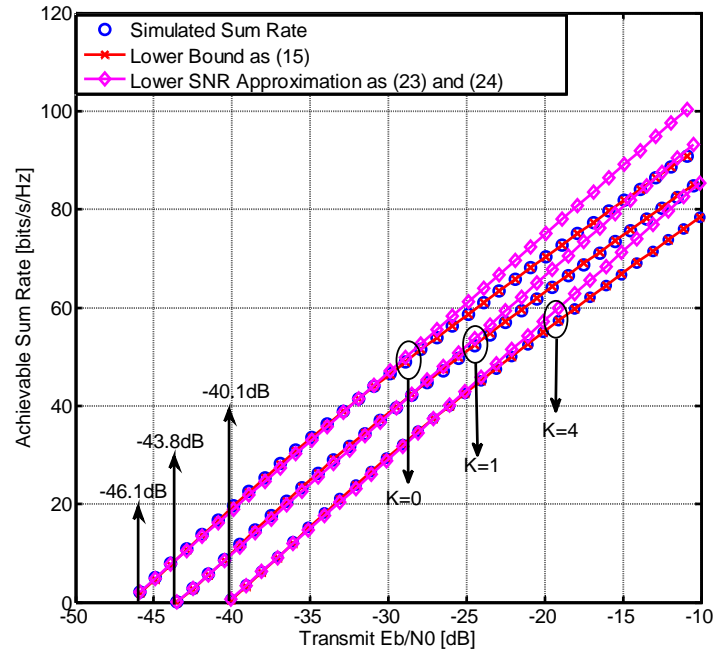


**Fig. 5.** Simulated sum rate, lower bound and low-SNR approximation versus the transmit energy per bit  $\frac{E_b}{N_0}$  in the low SNR regime ( $M = 10, N = 6, D = 400, \theta_{\text{init}} = 4^\circ$ )

## 5. Conclusion

This paper presented a detailed sum rate analysis of 3D-MIMO ZF receivers utilizing the BS antenna tilt angle in RC-LN fading channels. Specifically, closed-form lower bounds, high/low-SNR approximations on the sum rate were derived, which is applicable to the scenarios with arbitrary Ricean  $K$ -factor and is sufficiently tight across the entire BS antenna tilt angle and SNR regimes. In particular, the optimal BS antenna tilt angle to maximize the sum rate of the 3D-MIMO system was also obtained. More importantly, these analytical results encompass the small- and large-scale fading (include LN shadow fading, 3D antenna gain and path-loss) models of practical interest. Finally, we examined in detail (both theoretically and via numerical simulations) the impact of the Ricean  $K$ -factor, the radius of cell  $D$  and the BS antenna tilt angle  $\theta_{\text{init}}$  on the performance of system.

### Appendix A: Proof of Proposition 1

Substituting (11) and (13) into (14), we can obtain

$$\begin{aligned}
 \mathbf{R}(\theta_{\text{tilt}}, \gamma) &= \frac{1}{\ln 2} \sum_{n=1}^N \mathbb{E} \left[ \ln \left( 1 + \frac{\gamma [\boldsymbol{\Xi}]_{nn}}{N [(\mathbf{H}^H \mathbf{H})^{-1}]_{nn}} \right) \right] \\
 &= \frac{1}{\ln 2} \sum_{n=1}^N \mathbb{E} \left[ \ln \left( 1 + \frac{\gamma}{N} \exp \left( \ln([\boldsymbol{\Xi}]_{nn}) - \ln([(\mathbf{H}^H \mathbf{H})^{-1}]_{nn}) \right) \right) \right] \\
 &\stackrel{(a)}{=} \frac{1}{\ln 2} \sum_{n=1}^N \mathbb{E} \left[ \ln \left( 1 + \frac{\gamma}{N} \exp \left( \ln([\boldsymbol{\Xi}]_{nn}) + \ln(\det(\mathbf{H}^H \mathbf{H})) - \ln(\det(\mathbf{H}_n^H \mathbf{H}_n)) \right) \right) \right],
 \end{aligned} \tag{25}$$

where (a) is obtained by using the property of the matrix  $[\mathbf{A}^{-1}]_{nn} = \det(\mathbf{A}_{nn}) / \det(\mathbf{A})$  [20].

Exploiting the fact that  $\ln(1 + \alpha \exp(x))$  is convex in  $x$  for  $\alpha > 0$ , and applying Jensen's inequality, (25) can be lower bounded by

$$\begin{aligned}
 \mathbf{R}(\theta_{\text{tilt}}, \gamma) &\geq \mathbf{R}_L(\theta_{\text{tilt}}, \gamma) \\
 &= \frac{1}{\ln 2} \sum_{n=1}^N \ln \left( 1 + \frac{\gamma}{N} \times \exp \left( \mathbb{E} \left[ \ln([\boldsymbol{\Xi}]_{nn}) \right] \right. \right. \\
 &\quad \left. \left. + \ln(\det(\mathbf{H}^H \mathbf{H})) - \ln(\det(\mathbf{H}_n^H \mathbf{H}_n)) \right) \right).
 \end{aligned} \tag{26}$$

In RC-LN fading channel, we invoke the following results for an  $M \times N$  non-central Wishart matrix with rank-1 LoS component [22].

$$\mathbb{E} \left[ \ln(\det(\mathbf{H}^H \mathbf{H})) \right] = F(M, \Delta) - N \ln(K + 1) + \sum_{n=1}^{N-1} \psi(M - n). \tag{27}$$

Similarly,  $\mathbb{E} \left[ \ln(\det(\mathbf{H}_n^H \mathbf{H}_n)) \right]$  can be easily evaluated.

In addition, for the LN shadow fading terms, recall the fundamental properties of LN variation  $\xi_n \sim \text{LN} \left( \frac{\mu_n}{\eta}, \frac{\sigma_n^2}{\eta} \right)$  [23],

$$\mathbb{E} \left[ \xi_n^r \right] = \exp \left( \frac{r \mu_n}{\eta} + \frac{r^2 \sigma_n^2}{2 \eta^2} \right), \mathbb{E} \left[ \ln \xi_n \right] = \frac{\mu_n}{\eta}. \tag{28}$$

Combining (27) and (28), we can easily obtain (15).

### Appendix B: Proof of Theorem 1

From the low bound  $\mathbf{R}_L(\theta_{\text{tilt}}, \gamma)$  in (15), we can formulate the selection of BS antenna tilt angle as the following optimization problems:

$$\theta_{\text{tilt}}^* = \arg \max_{\theta_{\text{tilt}}} \mathbf{R}_L(\theta_{\text{tilt}}, \gamma). \tag{29}$$

Namely, the optimization problem of antenna tilt angle  $\theta_{\text{tilt}}$  is further written as

$$\theta_{\text{tilt}}^* = \arg \max_{\theta_{\text{tilt}}} \sum_{n=1}^N \ln(1 + b_n g_n(\theta_{\text{tilt}})), \quad (30)$$

where  $b_n = \frac{\gamma}{N} d_n^{-\nu} \exp\left(\frac{\mu_n}{\eta} + \psi(M - N + 1) + F(M, \Delta) - F(M, \Delta_1) - \ln(K + 1)\right)$ , To simply analyze, the optimization problem can be approximated as

$$\theta_{\text{tilt}}^* \approx \arg \max_{\theta_{\text{tilt}}} \sum_{n=1}^N \ln(b_n g_n(\theta_{\text{tilt}})). \quad (31)$$

The optimization problem can be further expressed as

$$\theta_{\text{tilt}}^* \approx \arg \max_{\theta_{\text{tilt}}} \sum_{n=1}^N \ln\{g_n(\theta_{\text{tilt}})\} + \ln b_n. \quad (32)$$

Due to  $G_m$ ,  $G_H(\theta_{\text{tilt}})$ ,  $\theta_{\text{3dB}}$  in  $g_n(\theta_{\text{tilt}})$  and  $b_n$  are constant, for sake of simplicity of expression, we focus only on the  $\theta_{\text{tilt}}$ -related part. The optimal antenna tilt angle  $\theta_{\text{tilt}}^*$  can be obtained

$$\theta_{\text{tilt}}^* \approx \operatorname{argmin}_{\theta_{\text{tilt}}} \sum_{n=1}^N (\theta_n - \theta_{\text{tilt}})^2. \quad (33)$$

Then, the solution of (33) is derived as

$$\theta_{\text{tilt}}^* \approx \sum_{n=1}^N \theta_n / N, \quad (34)$$

which is equal to the mean value of the vertical angles of the  $N$  users. This completes the proof.

## Appendix C: Proof of Proposition 2

For 3D-MIMO systems with ZF receivers, the slope and offset parameters are obtained by [19]

$$S_{\infty} = \min(M, N), \quad (35)$$

$$L_{\infty} = \frac{1}{\ln 2} \ln(N) - \frac{1}{N \ln 2} \sum_{n=1}^N \mathbb{E} \left[ \ln([\Xi]_{nn}) \right. \\ \left. + \ln(\det(\mathbf{H}^H \mathbf{H})) - \ln \det(\mathbf{H}_n^H \mathbf{H}_n) \right]. \quad (36)$$

Combining (27) with (28), (36) gives (20) after simplifications, we can conclude the proof.

## Appendix D: Proof of Proposition 3

First, we rewrite (14) as

$$\mathbf{R}(\theta_{\text{tilt}}, \gamma) = \frac{1}{\ln 2} \sum_{n=1}^N \mathbb{E} \left[ \ln \left( 1 + \frac{\gamma \xi_n g_n(\theta_{\text{tilt}}) d_n^{-\nu}}{N} x_n \right) \right], \quad (37)$$

where  $x_n = \frac{1}{[\mathbf{H}^H \mathbf{H}]_{nn}^{-1}}$ .

Note that  $\mathbf{H}^H \mathbf{H}$  follows a non-central Wishart distribution, denoted by  $\mathbf{H}^H \mathbf{H} \sim W_N(M, \mathbf{P}, \mathbf{\Sigma})$ , where  $\mathbf{\Sigma}$  is the covariance matrix of the row vectors of  $\mathbf{H}$ , i.e.,  $\mathbf{\Sigma} = \frac{1}{K+1} \mathbf{I}_N$  and  $\mathbf{P}$  is the mean matrix of  $\mathbf{H}$ , i.e.,  $\mathbf{P} = \sqrt{\frac{K}{K+1}} \mathbf{H}_L$  [23], which encumbers the derivation of  $E\left[\left[\left(\mathbf{H}^H \mathbf{H}\right)^{-1}\right]_{mm}\right]$ . Therefore, we resort to an increasingly popular approximation with a central Wishart distribution.

We can approximate  $\mathbf{H}^H \mathbf{H}$  by a central Wishart distribution with covariance matrix  $\hat{\mathbf{\Sigma}}$  as follows [25]

$$\begin{aligned} \hat{\mathbf{\Sigma}} &= \frac{1}{K+1} \mathbf{I}_N + \frac{K}{(K+1)M} \mathbf{H}_L^H \mathbf{H}_L \\ &= \frac{1}{K+1} \mathbf{I}_N + \frac{KN}{M(K+1)} \mathbf{a}_t^* \mathbf{a}_t^T, \end{aligned} \tag{38}$$

All principal diagonal elements of  $\hat{\mathbf{\Sigma}}$ ,  $\left[\hat{\mathbf{\Sigma}}\right]_{mm}$  are equal.  $x_n$  is a Chi-squared random variable with distribution as follows [26]:

$$f_{x_n}(x) = \frac{\left[\hat{\mathbf{\Sigma}}^{-1}\right]_{mm} e^{-x\left[\hat{\mathbf{\Sigma}}^{-1}\right]_{mm}}}{\Gamma(M-N+1)} \left(x\left[\hat{\mathbf{\Sigma}}^{-1}\right]_{mm}\right)^{M-N}. \tag{39}$$

By taking the first-order derivative of (37) with respect to  $\gamma \rightarrow 0$ , we can obtain

$$\begin{aligned} \dot{\mathbf{R}}(\theta_{\text{tilt}}, 0) &= \frac{1}{\ln 2} \sum_{n=1}^N E \left[ \frac{\frac{1}{N} \xi_n x_n d_n^{-\nu} g_n(\theta_{\text{tilt}})}{1 + \gamma \frac{1}{N} \xi_n x_n d_n^{-\nu} g_n(\theta_{\text{tilt}})} \Big|_{\gamma=0} \right] \\ &= \frac{M-N+1}{N \ln 2} \sum_{n=1}^N \frac{c_n}{\left[\hat{\mathbf{\Sigma}}^{-1}\right]_{mm}}. \end{aligned} \tag{40}$$

The expectation in (40) should be taken with respect to  $\xi_n$  and  $x_n$ . Similarly, we can obtain the second-order derivative of (37) with respect to  $\gamma \rightarrow 0$

$$\begin{aligned} \ddot{\mathbf{R}}(\theta_{\text{tilt}}, 0) &= -\frac{1}{\ln 2} \sum_{n=1}^N E \left[ \frac{\left(\frac{1}{N} \xi_n x_n d_n^{-\nu} g_n\right)^2}{\left(1 + \gamma \frac{1}{N} \xi_n x_n d_n^{-\nu} g_n\right)^2} \Big|_{\gamma=0} \right] \\ &= \frac{-(M-N+2)(M-N+1)}{N^2 \ln 2} \sum_{n=1}^N \frac{\exp\left(\frac{2\mu_n}{\eta} + \frac{2\sigma_n^2}{\eta^2}\right) g_n^2(\theta_{\text{tilt}})}{d_n^{2\nu} \left(\left[\hat{\mathbf{\Sigma}}^{-1}\right]_{mm}\right)^2}. \end{aligned} \tag{41}$$

Substituting (40), (41) into (22) and simplifying. The proof of the proposition is completed.

## References

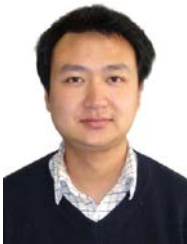
- [1] D. Gesbert, M. Kountouris, R. W. H. Jr., C. B. Chae, T. Salzer, "Shifting the MIMO Paradigm," *IEEE Signal Processing Magazine*, vol. 24, pp. 36–46, 2007. [Article \(CrossRef Link\)](#)
- [2] S. Vishwanath, N. Jindal, A. Goldsmith, "Duality, achievable rates, and sum-rate capacity of Gaussian MIMO broadcast channels," *IEEE Transactions on Information Theory*, vol. 49, pp. 2658–2668, 2003. [Article \(CrossRef Link\)](#)
- [3] 3GPP TR 36.814 V9.0.0, "Further advancements for E-UTRA physical layer aspects," *Technology Report*, 2010. [Article \(CrossRef Link\)](#)
- [4] X. W. Li, L. H. Li, L. Xie, "Achievable Sum Rate Analysis of ZF Receivers in 3D MIMO Systems," *KSII Transactions on Internet and Information Systems*, vol. 8, pp. 1368–1389, 2014. [Article \(CrossRef Link\)](#)
- [5] H. J. Liu, H. Gao, C. Zhang, T. J. Lv, "Low-Complexity Joint Antenna Tilting and User Scheduling for Large-Scale ZF Relaying," *IEEE Signal Processing Letter*, vol. 22, pp. 361–365, 2015. [Article \(CrossRef Link\)](#)
- [6] Q. T. Zhang, X. W. Cui, X. M. Li, "Very tight capacity bounds for MIMO-correlated Rayleigh-fading channels," *IEEE Transactions on Wireless Communications*, vol. 4, pp. 681–688, 2005. [Article \(CrossRef Link\)](#)
- [7] F. Q. Tan, H. Gao, T. J. Lv, J. Zeng, "Achievable Sum Rate Analysis of ZF Receivers in 3D MIMO with Rayleigh/Log-normal Fading Channels," in *Proc. of the IEEE GLOBECOM-Workshop*, Austin, TX, USA, pp. 900–905, 2014. [Article \(CrossRef Link\)](#)
- [8] D. Wang, J. Wang, Xiaohu You, Yan Wang, "Spectral efficiency of distributed MIMO systems," *IEEE Journal on Selected Areas in Communications*, vol. 31, pp. 2112–2127, 2013. [Article \(CrossRef Link\)](#)
- [9] M. Matthaiou, P. de Kerret, G. K. Karagiannidis, "Mutual Information Statistics and Beamforming Performance Analysis of Optimized LoS MIMO Systems," *IEEE Transactions on Communications*, vol. 58, pp. 3316–3329, 2007. [Article \(CrossRef Link\)](#)
- [10] G. Alfano, A. Lozano, A. M. Tulino, "Mutual information and eigenvalue distribution of MIMO Ricean channels," in *Proc. Of the IEEE ISITA*, Parma, Italy, pp. 2004. [Article \(CrossRef Link\)](#)
- [11] S. K. Jayaweera, H. V. Poor, "MIMO capacity results for Rician fading channels," in *Proc. of the IEEE GLOBECOM*, San Francisco, CA, USA, pp. 1806–1810, 2003. [Article \(CrossRef Link\)](#)
- [12] S. K. Jayaweera, H. V. Poor, "On the capacity of multiple-antenna systems in rician fading," *IEEE Transactions on Wireless Communications*, vol. 4, pp. 1102–1111, 2005. [Article \(CrossRef Link\)](#)
- [13] M. R. McKay, I. B. Collings, A. M. Tulino, "Achievable Sum Rate of MIMO MMSE Receivers: A General Analytic Framework," *IEEE Transactions on Information Theory*, vol. 56, pp. 396–410, 2010. [Article \(CrossRef Link\)](#)
- [14] I. S. Gradshteyn, I. M. Ryzhik, "Table of Integrals, Series, and Products," *Academic Press*, seventh edition, 2007. [Article \(CrossRef Link\)](#)
- [15] "Guidelines for evaluation of radio interface technologies for IMT-advanced," Geneva, Switzerland, Rep. M.2135-1, 2009. [Article \(CrossRef Link\)](#)
- [16] A. Yang, Z. W. He, C. W. Xing, Z. S. Fei, J. M. Kuang, "The Role of Large-Scale Fading in Uplink Massive MIMO Systems," *IEEE Transactions on Vehicular Technology*, 2015. [Article \(CrossRef Link\)](#)
- [17] Clerckx, Bruno, Claude Oestges. *MIMO Wireless Networks: Channels, Techniques and Standards for Multi-antenna, Multi-user and Multi-cell Systems*, Academic Press, 2013. [Article \(CrossRef Link\)](#)
- [18] Paulraj, Arogyaswami, Rohit Nabar, and Dhananjay Gore. *Introduction to space-time wireless communications*, Cambridge university press, 2003. [Article \(CrossRef Link\)](#)
- [19] S. S. Shitz, S. Verdú, "The impact of frequency-flat fading on the spectral efficiency of CDMA," *IEEE Transactions on Information Theory*, vol. 47, pp. 1302–1327, 2001. [Article \(CrossRef Link\)](#)
- [20] A. Lozano, A. M. Tulino, S. Verdú, "Multiple-antenna capacity in the low-power regime," *IEEE*



- Transactions on Information Theory*, vol. 49, pp. 2527–2544, 2003. [Article \(CrossRef Link\)](#)
- [21] Couillet R, Debbah M. *Random matrix methods for wireless communications*, Cambridge, MA: Cambridge University Press, 2011. [Article \(CrossRef Link\)](#)
- [22] S. Jin, X. Gao, X. You, “On the ergodic capacity of rank-1 Ricean fading MIMO channels,” *IEEE Transactions on Information Theory*, vol. 53, no. 2, pp.502–517, 2007. [Article \(CrossRef Link\)](#)
- [23] Simon M K, Alouini M S. *Digital communication over fading channels*. John Wiley & Sons, 2005. [Article \(CrossRef Link\)](#)
- [24] McKay, Matthew R., Iain B. Collings. “Statistical properties of complex noncentral Wishart matrices and MIMO capacity,” in *Proc. of the IEEE ISIT*, Adelaide, SA, pp. 785-789, 2005. [Article \(CrossRef Link\)](#)
- [25] Q. Zhang, S. Jin, K. K. Wong, H. B. Zhu, M. Matthaiou, “Power Scaling of Uplink Massive MIMO Systems with Arbitrary-Rank Channel Means,” *IEEE Journal of Selected Topics in Signal Processing*, vol. 8, pp. 966-981, 2014. [Article \(CrossRef Link\)](#)
- [26] D. A. Gore, R. W. Heath, A. J. Paulraj, “Transmit selection in spatial multiplexing systems,” *IEEE Communications Letters*, vol. 6, pp. 491–493, 2002. [Article \(CrossRef Link\)](#)



**Fangqing Tan** received the B.E degree in Electronics and Information Engineering from Hebei Polytechnic University in 2009 and received the M.S. degree in communication and information system from Chongqing University of Post and Telecommunications in 2012. He is currently pursuing the Ph.D. degree in Beijing University of Post and Telecommunications, Beijing, China. His research interests include Massive MIMO systems and digital signal processing in wireless communications.



**Hui Gao** received his B. Eng. degree in Information Engineering and Ph.D. degree in Signal and Information Processing from Beijing University of Posts and Telecommunications (BUPT), Beijing, China, in July 2007 and July 2012, respectively. From May 2009 to June 2012, he also served as a research assistant for the Wireless and Mobile Communications Technology R&D Center, Tsinghua University, Beijing, China. From Apr. 2012 to June 2012, he visited Singapore University of Technology and Design (SUTD), Singapore, as a research assistant. From July 2012 to Feb. 2014, he was a Postdoc Researcher with SUTD. He is now with the School of Information and Communication Engineering, Beijing University of Posts and Telecommunications (BUPT), as an assistant professor. His research interests include massive MIMO systems, cooperative communications, ultra-wideband wireless communications.



**Xin Su** received the M.S. and Ph.D. degrees in Electronic Engineering from UESTC (University of Electronic Science and Technology of China) in 1996 and 1999, respectively. Currently he is a full professor of the Research Institute of Information Technology in Tsinghua University. He is also the chairman of IMT-2020(5G) wireless technology work group in MIIT (Ministry of Industry and Information Technology of People's Republic of China) and vice chairman of the Innovative Wireless Technology Work Group of CCSA (China Communications Standards Association). His research interests include broadband wireless access, wireless and mobile network architecture, self-organizing network, software defined radio, and cooperative communications. Dr. Su has published over 100 papers in the core journals and important conferences, and owned more than 30 patents.



**Tiejun Lv** received the M.S. and Ph.D. degrees in electronic engineering from the University of Electronic Science and Technology of China (UESTC), Chengdu, China, in 1997 and 2000, respectively. From January 2001 to December 2002, he was a Postdoctoral Fellow with Tsinghua University, Beijing, China. From September 2008 to March 2009, he was a Visiting Professor with the Department of Electrical Engineering, Stanford University, Stanford, CA. He is currently a Full Professor with the School of Information and Communication Engineering, Beijing University of Posts and Telecommunications (BUPT). He is the author of more than 100 published technical papers on the physical layer of wireless mobile communications. His current research interests include signal processing, communications theory and networking. Dr. Lv is also a Senior Member of the Chinese Electronics Association. He was the recipient of the Program for New Century Excellent Talents in University Award from the Ministry of Education, China, in 2006.